Thin Solid Films 616 (2016) 828–837

Contents lists available at ScienceDirect

Thin Solid Films

journal homepage: www.elsevier.com/locate/tsf

Electrodeposition of Re-Ni alloys from aqueous solutions with organic additives

Wangping Wu [a], Noam Eliaz [a,*], Eliezer Gileadi [b]

[a] Biomaterials and Corrosion Laboratory, Department of Materials Science and Engineering, Faculty of Engineering, Tel-Aviv University, Ramat Aviv, Tel-Aviv 6997801, Israel
[b] School of Chemistry, Faculty of Exact Sciences, Tel-Aviv University, Ramat Aviv, Tel-Aviv 6997801, Israel

ARTICLE INFO

Article history:
Received 15 April 2016
Received in revised form 27 September 2016
Accepted 5 October 2016
Available online 6 October 2016

Keywords:
Electrodeposition
Bath additives
Nickel
Rhenium
Surface cracking

ABSTRACT

In this study, Re-Ni alloys with high Re content were electrodeposited on copper substrates from aqueous solutions containing additives with a combination of vanillin, sodium lauryl sulfate and gelatin. The bath additives were found to have a significant effect on the chemical composition, surface morphology and cracking pattern. The morphology of the alloy was changed from uniformly smooth without additives to relatively coarse-grained with three additives. The deposition rate and crack density decreased when additives were added to a bath containing 34 mM ReO_4^-, 124 mM Ni^{2+} and 343 mM $[Cit]^{3-}$. Almost pure Re films were formed at low Ni^{2+} concentration of 30–50 mM due to the effect of additives; however, the deposited film was thin. A thin layer of Re oxide, a new Re-O-C-complex state and some organic residues from additives were formed at the surface of the Re film. Both the Re-rich alloy and the Re film were found to have an amorphous structure.

1. Introduction

Rhenium (Re) is a refractory metal with a unique combination of properties that makes Re and its alloys attractive for a variety of high-temperature, catalytic, energy, electrical and biomedical applications, in spite of its high cost [1–3]. At present, the main manufacturing processes for Re and its alloys are powder metallurgy [1,2] and chemical vapor deposition [3], and to a lesser extent – electroless plating [4–6] and electrodeposition [7–27].

Re belongs to a group of metals that are difficult to deposit from aqueous solutions [11]. Previous work in our laboratory has found that the addition of one of the iron-group metals (Ni, Co, or Fe) to the solution bath leads to high Faradaic efficiency (FE) and high Re-content in the deposits. This catalytic effect of iron-group metals on Re electrodeposition, as well as the mechanism of codeposition has been investigated in detail in our lab in recent years [11–14,19–21]. The Re-Ni alloy system is of particular interest because of the extensive mutual solubility of Re and Ni and the absence of intermetallic compounds in the Re-Ni peritectic phase diagram.

In our previous work, the effects of bath chemistry and deposition time on the FE, composition and partial deposition current densities were systematically studied [11–14]. It was found that the addition of a Ni salt to a bath containing ReO_4^- resulted in coatings with high Re-content (up to 93 at.%), high FE (up to 96%), and a thickness as high as 25 μm, with potential for depositing even thicker layers at longer deposition times.

To date, only few publications have dealt with the influence of bath additives on electrodeposited Re-Ni alloys, possibly due to the confidentiality of many related projects worldwide. Only a limited number of scientific and technical publications [8,27,28] discuss the addition of additives to solutions for Re-Ni alloy electrodeposition. Nano-grain Re-Ni alloys with low Re-content (<35 at.%) was electrodeposited onto stainless steel from sulfamate-based electrolytes containing wetting agents, stress reducers and brighteners, but the specific nature of the chemicals used was not disclosed [27]. Greco [8] reported that fine hairline cracks appear on the surface of Re-Ni alloys with low Re-content (lower than 16 at.%) when electrodeposited with a sodium lauryl sulfate (SLS). Huang et al. [28] studied electroformed crack-free Ni-rich Re-Ni alloys by adding $KReO_4$ to the nickel bath and employing saccharin.

In the current study, the Re-rich alloys were electrodeposited galvanostatically from aqueous solutions with combination of vanillin (Van), SLS and gelatin (Gel) as additives. Sodium lauryl sulfate ($H_3C(CH_2)_{11}OSO_3N/a$), a well-known wetting agent, is known to prevent hydrogen bubbles from adhering to the cathode surface. As-deposited Re is not stable in moist air [1]. Metallic Re has low hydrogen overpotential, and absorption of hydrogen can result in hydrogen embrittlement [29]. Therefore, we chose the SLS additive to study the properties of the deposits. Gelatin, a leveling agent, is known to improve the morphology of the deposits through adsorption onto active growth sites, thus controlling the deposition rate [30,31]. Vanillin ($C_8H_8O_3$) is often used as a brightener. All the three additives were included in an

* Corresponding author.
E-mail address: neliaz@tau.ac.il (N. Eliaz).

http://dx.doi.org/10.1016/j.tsf.2016.10.012
0040-6090/

effort to track synergistic effects between the additives on the properties of the deposits. The main objective of the current work was to investigate the effects of additives, bath chemistry and operating conditions on the FE, partial current densities, chemical composition, and surface morphology of Re-rich Re-Ni alloy deposits.

2. Experimental details

2.1. Bath chemistry

In this study, Re-Ni alloys were electrodeposited from aqueous solutions containing 34–94 mM NH_4ReO_4, 34–155 mM $Ni(NH_2SO_3)_2$ and 100–343 mM citric acid. In most cases, the composition of the electrolyte was 34 mM NH_4ReO_4, 124 mM $Ni(NH_2SO_3)_2$ and 343 mM citric acid. The additives were 1 mM Vanillin (Van), 1 mM sodium lauryl sulfate (SLS), and 2 g L^{-1} gelatin (Gel).

2.2. Procedure

A three-electrode cell was used. A copper disc cathode with an exposed surface area of 1.57 cm^2 served as the working electrode, two platinum sheets placed approximately 0.5 cm on both sides of the WE served as the counter electrodes, and the reference electrode was Ag/AgCl/KCl(sat.). Prior to electrodeposition, the surface of the copper substrate was cleaned with a detergent in an ultrasonic bath for 5 min, and then immersed in a 1:1 solution of 70 wt.% nitric acid in deionized water at room temperature for about 1 min, to remove the native oxide films on the surface of the copper substrate. This was followed by another cleaning with acetone in an ultrasonic bath for 3–5 min. In most cases, the deposition conditions of Re-Ni alloy were as follows: current density of 50 mA cm^{-2}, pH = 5 ± 0.1, and bath temperature 70 ± 1 °C. The volume of the electrolyte in the cell was approximately 10 mL. The deposition process was typically run for 60 min, although the shortest deposition time was 10 min. Some experiments were carried out at pH values varying from 3 to 9, or at temperatures of 50–80 °C.

A Princeton Applied Research model 263 A Potentiostat/Galvanostat was used to control the applied current density. A thermostatic bath (MRC, B300) was used to control the bath temperature. All solutions were prepared with deionized water (Direct-Q3, Millipore, theoretical resistivity 18.2 MΩ cm). A 5 M sodium hydroxide solution was used to adjust the pH to the chosen value. When Gel additive was added, the solution was heated to 50–60 °C and stirred by a magnetic stir bar for 30–40 min in order to maintain solution homogeneity. The solution was then cooled to room temperature for pH adjustment, and then heated again for 15–20 min. The bath was purged with pure nitrogen for 15 min before turning on the current. A nitrogen blanket was passed above the solution during deposition.

The mass gain due to alloy deposition was tracked with an analytical balance (BA 210 from Sartorius, resolution 0.1 mg) before and after each experiment. The average FE was calculated from the added mass, the charge passed and the chemical composition of the alloy. The partial current densities of the two metals were calculated from the added mass and the chemical composition of the alloy. Further details can be found in our previous publication [11].

2.3. Characterization

Both the top surface and cross-section of the Re-Ni coatings were imaged by an environmental scanning electron microscope (ESEM, Quanta 200 FEG from FEI) at 12.5 keV and a working distance of 10 mm, operated in the high-vacuum mode. The attached liquid-nitrogen-cooled Oxford Si energy-dispersive spectroscopy (EDS) detector was used to determine the surface composition of the alloy. The energy of the primary electrons was 20 keV. Each sample was tested at five locations to confirm uniformity.

The phase of the alloy was determined by X-ray powder diffraction (XRD, Scintag, USA) equipped with a liquid-nitrogen-cooled germanium solid-state detector and a Cu-K_α radiation source. X-ray photoelectron spectroscopy (XPS) measurements were performed in ultrahigh vacuum (3.3×10^{-8} Pa base pressure) using a 5600 Multi-Techniques System (PHI, USA). The samples were irradiated with an Al-K_α monochromatic source (1486.6 eV), and the outcome electrons were analyzed by a Spherical Capacitor Analyzer using the slit aperture of 0.8 mm. The samples were analyzed either at the surface or after sputter cleaning with a 4 kV Ar^+ ion gun (sputtering rate on SiO_2/Si was 3.3 nm min^{-1}). The carbon signal for C1 s at 285 eV was taken as an energy reference for the measured peaks. In order to identify the elements present at the surface of the film, a low-resolution survey spectrum was first taken over a wide energy range (0–1400 eV). High-resolution spectra were acquired at pass energy of 11.75 eV at increments of 0.05 eV $step^{-1}$, to allow precise determination of the position of the peaks and their shape. Curve-fitting was done with Gaussian–Lorentzian function, using the 5600 Multi-Technique System software. Two fitting parameters – the position of the peak and its full width at half maximum – were fixed within less than about ±0.2 eV.

3. Results and discussion

In the framework of this work, samples were electrodeposited from solutions with the same composition of additives, and at the same time with different bath chemistries and operating conditions. Section 3.1 shows the effects of the concentrations of perrhenate, nickel and citrate ions on the FE and Re-content in the alloy, in the presence of additives. The effects of pH and temperature when additives are present are discussed in Sections 3.2 and 3.3, respectively. Section 3.4 shows the surface morphology, cracking pattern and chemical composition of representative alloy deposits. Finally, the crystallographic structure of the alloys is analyzed in Section 3.5. The bath composition for representative samples for discussion is listed in Table 1.

3.1. The effects of the perrhenate, nickel and citrate concentrations

Fig. 1 shows the effect of ReO_4^- concentration on the main deposit properties, for $Ni[(SO_3)(NH_2)]_2$ concentrations ranging from 34 to 155 mM. Considering this figure, the following trends become apparent:

1. As the concentration of Ni^{2+} in the electrolyte is increased, the Re-content in the alloy decreases (Fig. 1(a)), while the partial current density for the deposition of Ni increases (Fig. 1(d)). It should be noted that the total applied current is constant throughout the experiments, and Ni and Re ions are each partaking in competing reactions. The FE (Fig. 1(b)) also increases with increasing Ni^{2+} concentration. This can be understood by considering that Re is a better catalyst for hydrogen evolution

Table 1
Bath compositions and additive concentrations for selected samples.

Sample	NH_4ReO_4 (mM)	$Ni(NH_2SO_3)_2$ (mM)	$C_6H_8O_7$ (mM)	Figure
Ref. [11]*	34	124	343	6a, 11a
#67	34	124	343	6b, 7a, 11b
#82	94	124	343	6c
#85[@]	34	124	343	6e
#86[@@]	34	124	343	6f
#72	34	124	100	6d
#125	50	50	343	6g, 7b, 8–10, 11c

Note: Bath temperature 70 °C, current density 50 mA cm^{-2}, pH = 5. All depositions were conducted for 60 min. The concentrations of Van, SLS and Gel were 1 mM, 1 mM and 2 g L^{-1}, respectively. *No additives were added. [@] pH = 9, [@@] Bath temperature 80 °C.

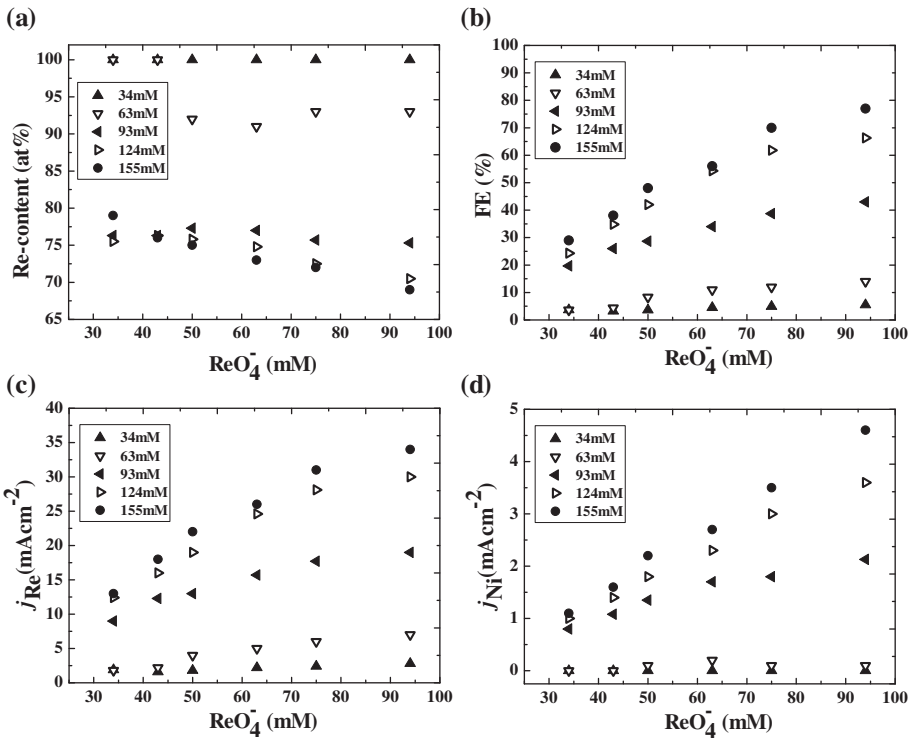

Fig. 1. Plots of the Re-content (a), the FE (b), the partial current density of Re (c), and the partial current density of Ni (d) as a function of the concentration of ReO_4^-, with different concentrations of $Ni[(SO_3)(NH_2)]_2$. The concentration of citric acid: 343 mM.

than Ni. Therefore, as the Re-content in the alloy declines, the competing hydrogen evolution reaction declines as well, thus leading to an increase in the FE.

2. Interestingly, as the concentration of $Ni[(SO_3)(NH_2)]_2$ is increased, the partial current density for deposition of Re increases as well (Fig. 1(c)). This confirms the claim in earlier publications from our laboratory that Ni ions catalyze the electrodeposition of Re [11–14].
3. The question of ReO_4^- ion's capability to catalyze Ni deposition is slightly more difficult to see in Fig. 1(d). This is due to the fact that at low concentrations of $Ni[(SO_3)(NH_2)]_2$, the partial current density for Ni deposition is quite low (due to high sequestering of nickel ions by a large excess of citrate ions, as will be shown below). However, when the Ni concentration falls within the range of 93–155 mM, this catalysis can be clearly seen.
4. Finally, an interesting observation can be made from Fig. 1(a-d) regarding the complexing properties of Ni^{2+} with species derived from citric acid. Nickel can exist in solution either as free hydrated Ni^{2+} ions, as $[NiCit]^-$, or as $[NiCit_2]^{4-}$ [32]. The most significant factor in determining the complexes present is the ratio between the stoichiometric concentrations of citrate and Ni. It is well known that the rate of deposition of the free nickel ion is faster than that of a nickel-citrate ion. Likewise, Ni-deposition is blocked almost completely when there is a large excess of $[NiCit_2]^{4-}$. Thus, one can expect to observe a change at the point where free hydrated Ni^{2+} ions are exhausted. In Fig. 1 we used five concentrations, and there is a clear separation between the two lower concentrations of $Ni[(SO_3)(NH_2)]_2$ (34 and 63 mM) and the two higher concentrations (124 and 155 mM). The data for 93 mM fall roughly in the middle between the two groups. Therefore, it is proposed that around the concentration of 93 mM of $Ni[(SO_3)(NH_2)]_2$, free hydrated Ni^{2+} ions begin forming in the solution. Indeed, there is very little deposition of metallic nickel at the two lowest concentrations of Ni, and the Re-content is close to 100%. Unfortunately, the FE in such electrolytes is also very low, making such a system unlikely to be used for practical applications.

Fig. 2 shows the dependence of the Re-content, FE and partial current densities of Re and Ni on the Ni^{2+} concentration. The

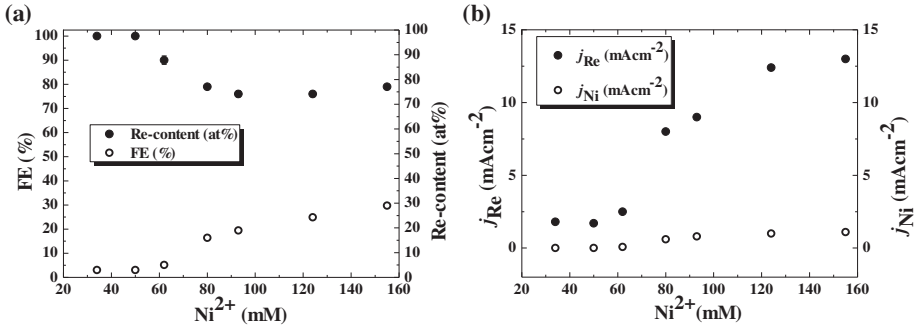

Fig. 2. Same as Fig. 1, but plotted here as a function of the Ni^{2+} concentrations in solution. The concentrations of ReO_4^- and citric acid in the plating baths were 34 mM and 343 mM, respectively.

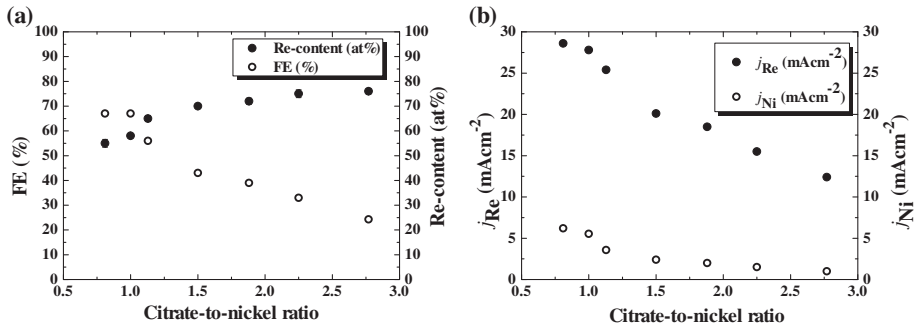

Fig. 3. Same as Fig. 1, but plotted here as a function of the concentration of citric acid. The concentrations of ReO_4^- and Ni^{2+} in the plating baths were 34 mM and 124 mM, respectively.

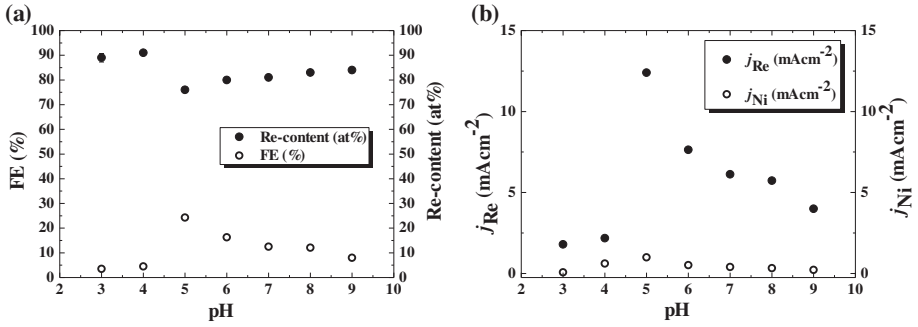

Fig. 4. Same as Fig. 1, but plotted here as a function of pH. The concentrations of ReO_4^-, Ni^{2+} and citric acid in the plating baths were 34 mM, 124 mM and 343 mM, respectively.

concentrations of ReO_4^- and citric acid in the plating baths were 34 mM and 343 mM, respectively. It can be seen from Fig. 2(a) that the Re-content in the deposits decreases dramatically as the Ni^{2+} concentration increases from 50 to 80 mM, but decreases slightly and seems to remain constant with further increasing concentration of Ni^{2+}. The FE for electrodeposition steadily increased from 3% to 29% as Ni^{2+} concentration increased from 34 to 155 mM. It should be noted that Re films were obtained at low concentration of Ni^{2+} ion (34–50 mM), corresponding to the lowest FE of 3%. Although increasing the Ni^{2+} concentration led to a decrease in Re-content in the alloys, it caused a steady increase in the partial current density of Re, as well as a slight increase in that of Ni (see Fig. 2(b)). Therefore, it can be said that the presence of nickel in solution catalyzed the deposition of Re.

Netherton and Holt [7] investigated the effect of the Ni^{2+} concentration in citrate baths on both the Re-content in the alloy and on the FE. They found that the Re-content decreased with increasing concentration of Ni^{2+}, while the FE increased to a maximum and then decreased somewhat. Naor et al. [11] reported that under the same conditions and with the same ReO_4^- and citric acid concentrations but without additives, Re-Ni alloy deposition showed a similar behavior. The results showed the highest Re-content in the alloys (93 at.%) at low Ni^{2+} concentrations (34–50 mM). In the present work, a Re deposit was obtained at low concentrations of Ni^{2+}, which was attributed to the effect of additives. The increase in the Re-content due to the additives will be discussed further in Section 3.4.

Fig. 3 shows the effect of the citric acid concentration on the properties of the Re-Ni deposits. The concentrations of ReO_4^- and Ni^{2+} in these experiments were 34 mM and 124 mM, respectively. In Fig. 3(a), the Re-content in the alloy is seen to increase steadily, while the FE remains constant between citric acid concentrations of 100 to 124 mM, and then decreases from 67% to 25% with further increase in citric acid concentration. The distribution of the citrate-containing species at this pH is 11.6% [$(H_2Cit)^-$], 67.7% [$(HCit)^{2-}$], and 20.7% [$Cit]^{3-}$, with each species affecting the deposition process in a different manner. The most abundant Ni-citrate complex, however, is $(NiCit)^-$, apparently due to the higher stability of the positive Ni^{2+} ion with the three negative charges on Cit^{3-}. With this in mind, one can suggest that the increase in the Re-content in the alloy as citric acid concentration increased is related to the

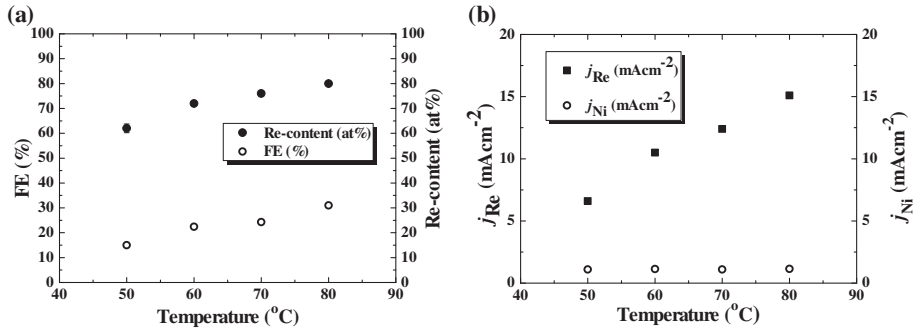

Fig. 5. As in Fig. 4, but plotted here as a function of bath temperature.

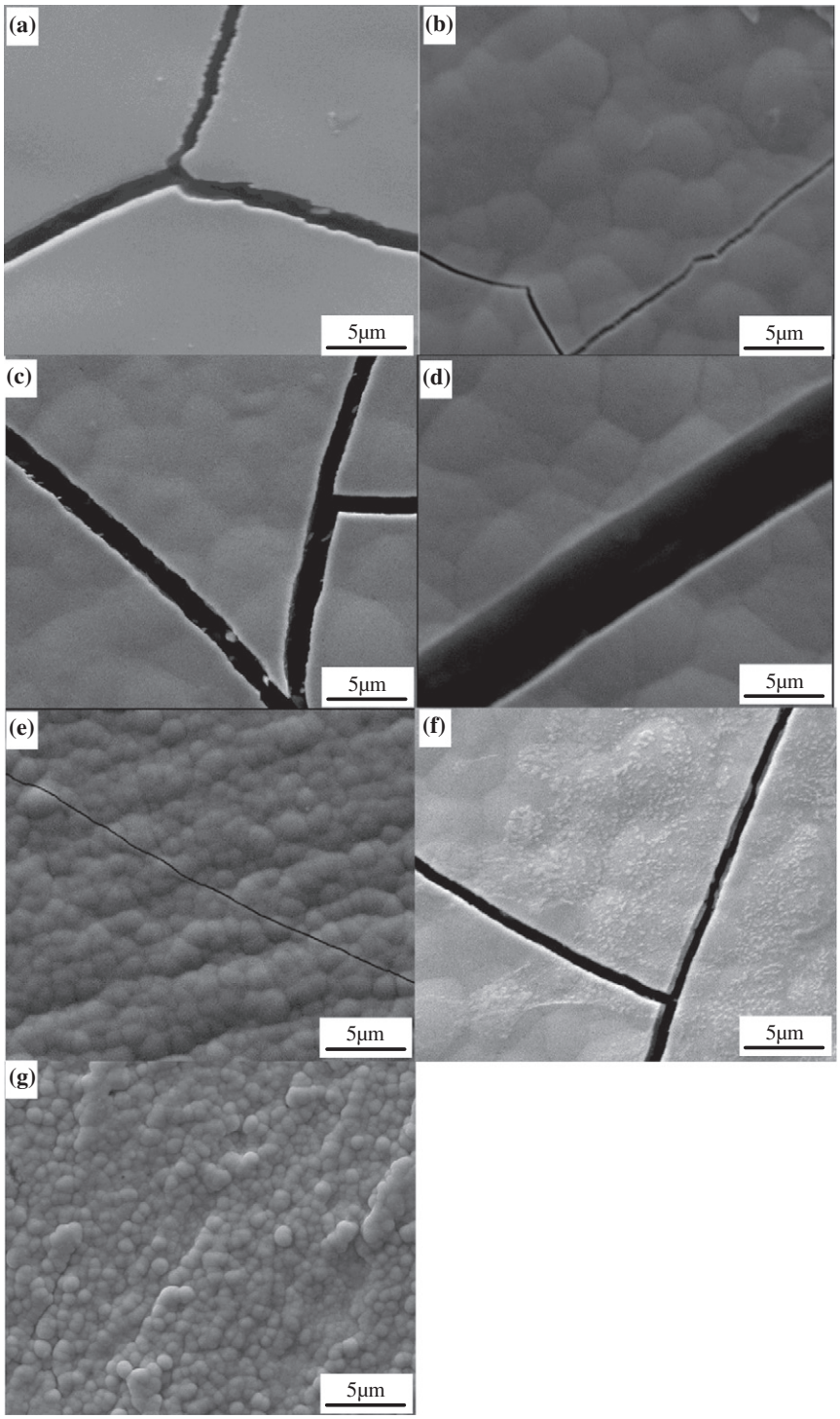

Fig. 6. ESEM images taken from seven Re-Ni alloy deposits on copper substrates, representing different process parameters and additives. See text for details. The samples are: (a) No additive, (b) #67, (c) #82, (d) #72, (e) #85, (f) #86, and (g) #125 (cf. Table 1).

formation of a Ni-deposition inhibiting species. Since Ni^{2+} acts as a catalyst for deposition of Re, the partial current densities for both Ni and Re were found to decline as the citrate/Ni ratio increased, as seen in Fig. 3(b).

3.2. The effect of pH

The dependence of the parameters of deposition on pH is illustrated in Fig. 4. All electrolytes consisted of 34 mM NH_4ReO_4, 124 mM $Ni[(SO_3)(NH_2)]_2$ and 343 mM citric acid. Fig. 4(a) shows that the highest Re-content (91 at.%) was obtained when the pH was 4, corresponding to a very low FE (4.5%). In contrast, at pH = 5, the highest FE (24.3%) and partial current density (12.4 mA cm^{-2}) of Re were obtained, while the Re-content (76 at.%) was the lowest (see Fig. 4(b)). The correlation between high Re-content and low FE (and vice versa) has been reported in previous studies where no additives were used [11]. Considering that in most cases, the effects of these additives are via adsorption on the surface of the substrate, their pH-dependence is therefore not surprising. Fig. 4 shows that the FE is very low at a pH of 3 and 4, and similarly at a pH or 8 and 9. Thus, at low pH values this

Table 2
Characteristics of selected samples. *w* is the added mass.

Sample	*w* (mg)	Re (at.%)	Ni (at%)	FE	Thickness* (μm)
Ref. [11]	45.3	60	40	57	16.0 ± 0.1
#67	19.1	76	24	24	9.3 ± 0.3
#82	54.5	67	33	69	31.6 ± 0.2
#72	53.2	55	45	67	34.5 ± 0.9
#85	6.2	84	16	8	5.1 ± 1.0
#86	24.5	80	20	31	16.6 ± 0.4
#125	3.1	100	0	4	1.4 ± 0.1

* The average thickness was measured on the cross-sections of the coatings.

system is not likely to be of any practical interest, in spite of the fact that Re film can be deposited. However, at pH 5, the Re-content is above 70 at.%, and the FE value somewhat above 20%. Therefore, this could prove to be a reasonable pH for deposition of high Re-content alloys. Moreover, reducing the Ni-content of the bath, while maintaining the pH value of 5, could lead to deposition of alloys having a higher Re-content, without decreasing the FE.

Netherton and Holt [7] and Fukushima et al. [9] studied the effect of pH on Re-content and FE for Re-Ni alloys in the absence of additives. The results obtained were similar, yet not identical to our results shown here. We attribute the differences to the effect of the additives, in particular the dependence of the extent of adsorption, and possibly to change of the structure of the adsorbed additives with pH.

3.3. The effect of bath temperature

The temperature-dependence of the FE and the Re-content in the deposit is displayed in Fig. 5. The bath composition and parameters measured are as in Fig. 4, the pH was 5.0 ± 0.1. It can be noted from Fig. 5(a) and (b) that the FE, Re-content, and partial current density of Re increased steadily with increasing temperature from 50 °C to 80 °C, as expected. The temperature dependence of the formation of electrodeposited Re-Ni alloys without additives has been studied in earlier works [7,33]. Eliaz et al. [34] observed a similar behavior for alloys of Zn-Ni, Zn-Co and Zn-Ni-Co. The interpretation of the data is very difficult in the case of an alloy, as there are at least two reactions taking place simultaneously, and several equilibria are involved (e.g. formation of Ni^{2+} and citrate complexes). Each rate constant and equilibrium constant could depend differently on temperature, plus the extent of adsorption may also be temperature-dependent.

3.4. Surface morphology, cracking pattern and chemical composition

Fig. 6 shows ESEM images acquired from seven Re-Ni alloys associated with different parameters and additives. Characteristics of selected samples are summarized in Table 2. Fig. 6(a) shows an ESEM image of the surface of the alloy deposited without additives. The composition of the electrolyte is as in Fig. 4. The Re-content and the FE were 60 at.% and 57%, respectively. Large cracks are observed, but the rest of the surface is very smooth. These cracks may result from volumetric changes due to hydrogen absorption during electrodeposition, from hydride decomposition shortly after electrodeposition, or from residual stresses due to formation of several phases with different lattice parameters within the coating [1, 26]. The deposition rate of the Re-Ni alloy deposited without additives was approximately 16 μm h^{-1} (See Table 2).

Fig. 6(b) shows the surface morphology of sample #67. The composition of the electrolyte was as in Fig. 4. The Re-content and the FE for this sample were 76 at.% and 24%, respectively. The surface morphology of the alloy consists of many colonies with non-uniform dimensions. The crack width decreased significantly with the use of additives, and the cracks cross through colonies. It is thus concluded that the addition of three additives has a significant effect on the chemical composition, surface morphology and crack density of the Re-Ni deposits. The thickness of this deposit was 9.3 ± 0.3 μm (Fig. 7(a)). The deposition rate of the coating decreased with addition of additives in the solutions.

Fig. 6(c) demonstrates the surface morphology of sample #82. The composition of the electrolyte was the same as in Fig. 4, except that the concentration of ReO_4^- was increased to 94 mM. The Re-content and the FE for sample #82 were 67 at.% and 69%, respectively. The thickness of this deposit was quite high (31.6 ± 0.2 μm), in spite of the significantly increased ReO_4^- concentration (from 34 to 94 mM). This supports our earlier findings [11] that the rate of deposition of Re is independent of the concentration of the perrhenate ion, with the exception of extremely low concentrations where mass transport of ReO_4^- becomes partially rate determining. The surface of the alloy seems to be smoother than in Fig. 6(b), and contains relatively large microcracks. Increasing the concentration of ReO_4^- led to a major increase in the width of the cracks, when compared to Fig. 6(b).

Fig. 6(d) demonstrates the surface morphology of sample #72. The composition of the electrolyte was the same as in Fig. 4, except that the concentration of citric acid was decreased to 100 mM. The Re-content and FE for sample #72 were 55 at.% and 67%, respectively. The reduction of the concentration of citric acid (from 343 to 100 mM) led to an increase in the concentration of free hydrated Ni^{2+} ions. A comparison of samples #82 and #72 indeed shows a reduction of the Re-content in the alloy and an increase in the Ni-content. The FE is almost the same, as is the thickness. Unfortunately, after deposition, most of the deposit delaminated from the substrate. The deposit was brittle, and large cracks were formed on its surface. This is most likely due to the fact that the citrate concentration was lower than that of the Ni^{2+} ion. Naor et al. [11] reported that at a Cit/Ni ratio < 1, free hydrated Ni^{2+} and $[NiCit]^-$ are the predominant species. As this ratio reaches unity, the concentration of free hydrated Ni^{2+} falls almost to zero, whereas a further increase in the concentration of citrate leads to the formation of complexes such as $[(Ni)(H_2Cit)_2]^0$ or $[(Ni)(HCit)_2]^{2-}$.

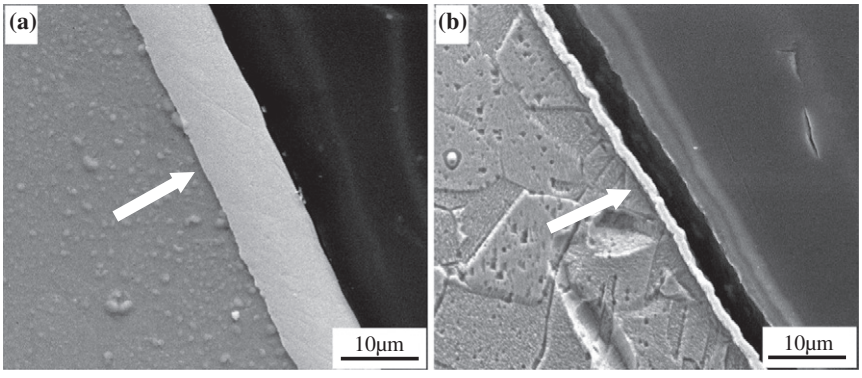

Fig. 7. ESEM images of metallographic cross-sections of three Re-Ni alloys. Coating (see arrow) thickness is given in the text. The samples are: (a) #67, (b) #125.

Table 3
Atomic composition (at%) of sample #125 before and after sputtering, as determined by XPS.

	Before sputtering	5 min sputtering	10 min sputtering
C	42.7	4.9	5.2
O	27.7	4.7	5.2
Re	12.4	86.4	86.0
Cu	1.4	0.4	0.4
N	11.4	2.9	2.7
Na	4.4	–	–
Ni	–	0.7	0.5

These complexes can sequester the Ni^{2+} ion, thus inhibiting its reduction. The rate of Ni deposition is therefore expected to decrease in the order of $Ni^{2+} > NiCit^{-} > NiCit_2{}^{4-}$, both at pH = 5 and at pH = 8. This explains the decrease in Re-content and increase in Ni-content in the present work. Thus, the ratio between the concentrations of citric acid, Ni^{2+} and ReO_4^- in solution is an important factor in controlling the deposition rate, FE and composition of the alloy in the Re system.

Fig. 6(e) shows the surface morphology of sample #85. The composition of the electrolyte was the same as in Fig. 4, with the exception that the pH was 9. The Re-content and the FE were 84 at.% and 8%, respectively. The surface of the deposit consists of many colonies with uniform dimensions. The size of the colonies is much smaller than in Fig. 6(b). The width of cracks decreased slightly in comparison with Fig. 6(b). The thickness of the deposit at pH = 9 was low (5.1 ± 1.0 μm), corresponding to the very low FE.

Fig. 6(f) shows the surface morphology of sample #86. The composition of the electrolyte was the same as in Fig. 4, except that the bath temperature was increased from 70 °C to 80 °C. When compared with Fig. 6(b), the increase in bath temperature is seen to have resulted in an increase of both the Re-content and the FE. In addition, cracks with many nanoparticles of Re and Ni were formed on the surface. Although nanoparticles are evident at high magnification within each colony in Fig. 6(b-e), they are more pronounced in Fig. 6(f). The consequence of temperature changes on the quality of the deposit is hard to predict, as discussed above (cf. Section 3.3). Considering that the reduction of the ReO_4^- ion is not the rate determining step, it may be suggested that increasing the temperature would shift the equilibrium between the Ni-citrate complexes in the direction of releasing more free hydrated Ni^{2+}, which then acts as a catalyst for the reduction of the ReO_4^- ion. The thickness of the deposited layer is reduced by a factor of about two, compared to samples #82 and #72 (Fig. 6(c) and 6(d), respectively).

Fig. 6(g) shows the surface morphology of sample #125. The composition of the electrolyte was the same as in Fig. 4, except that the concentrations of both ReO_4^- and Ni^{2+} were both 50 mM. The Re-content and the FE were 100 at.% and 4%, respectively. Under these deposition conditions, a black Re film was formed. The surface morphology of the film was composed of many small spherical globules, and very thin cracks are seen along the boundaries on the surface. Fig. 7(b) shows that the thickness of this film was about 1.4 μm. The coating is not straight and uniform. According to Fig. 1(a), Re films were obtained at low concentrations (34 and 50 mM) of Ni^{2+} while keeping the other components constant, but the FE was only 3%. The highest Re-content (93 at.%) obtained in the absence of additives was found in alloys deposited from the baths with low concentrations (34 and 50 mM) of Ni^{2+}. However, the FE in such instances was only 11–12% [11]. With addition of 1 mM Van, 1 mM SLS and 2 g L^{-1} Gel to equal concentrations of Ni^{2+} and ReO_4^-, Re film was formed. In many other cases, we found that the surface of Re-Ni alloys with 90–100 at.% Re consisted of very small, or even no cracks, but the FE was very low.

Organic additives adsorbed on the surface of metal cathode could affect the activation energy, the mechanism of electrocrystallization, and the rates of mass transport and charge transfer in the electrochemical reaction [35,36]. Additives are added to a plating bath for a number of purposes, including controlling hydrogen evolution, crystal texture, grain size and roughness, as well as to reduce residual stresses, increase hardness, and impart a mirror-like luster to the surface. Franklin [37] reviewed some mechanisms by which additives could affect the rate of metal electrodeposition. In the current work, SLS is a well-known wetting agent, which could prevent hydrogen bubbles from adhering to the metal cathode surface. It could act by the mechanism of hydrogen absorption. The molecular structure of Gel consists of a series of amino acids linked to one another via peptide bonds. In the electrolyte, several nitrogen atoms are available for adsorption on the electrode surface, and form complexes with metal ions. Brown and Hope [38] reported that adsorption of Gel on the cathode surface occurs through electron-rich donor atoms such as nitrogen. The chemical environment of each of these nitrogen atoms is influenced by neighboring functional groups and the extent of hydrogen bonding in the molecule. Gelatin was found to suppress the growth of nuclei through preferential adsorption on the cathode surface. Kostromina et al. [39] suggested that Ni^{2+} displays a strong tendency to form bonds with NH groups in a bath containing Gel at pH of 3.0–5.0. The lack of Ni deposition may be explained by assuming that the complexes formed with Ni ions suppressed the reduction of Ni ions in the electrolyte or controlled the transport of Ni ions. The mechanism by which Gel affects the electrodeposition could be adsorption of ligand complexes with the metal ion which increases the amount of metal ion adsorbed on the electrode (thus increasing the rate of reduction), or the ability of a complexed ion to accelerate the rate of electrons transfer from the electrode to the metal ion through the additive. Vanillin is used as a brightener. In leveling and brightening mechanisms there is a debate on whether additive adsorption is on active sites, geometrical protrusions or specific crystallographic faces, and whether the influence is on diffusion or deposition, but there is general agreement that the additive is essentially acting only as an impurity [37]. In our study, the mixture of all three additives led to no evidence of Ni deposition, determined by EDS pattern. In citrate solutions without Gel, high citric acid concentrations led to an increase in Re-content. This is perhaps related to the formation of $[Ni(H_2Cit)_2]^0$ or $[Ni(HCit)_2]^{2-}$, which inhibit parallel paths for deposition of Ni [11].

The chemical composition of sample #125 was analyzed by XPS. The atomic composition of the alloy before and after 5–10 min sputtering is listed in Table 3. Before sputtering, the elements C, O, N, Re, Cu and Na were identified at the surface. The small amount of Cu is likely due to inhomogeneities in the thin film, and therefore slight exposure of the substrate. After sputter cleaning, Na disappeared, and C, O and N decreased significantly. This is to be expected for C, O and N when present due to either ordinary adsorption from the environment or adsorption of organic additives on the cathode surface during electrodeposition. It should be noted that a small amount of Ni appeared following sputter cleaning, and the concentration of Re increased remarkably (see Fig. 8). It appears, therefore, that a thin layer of Re

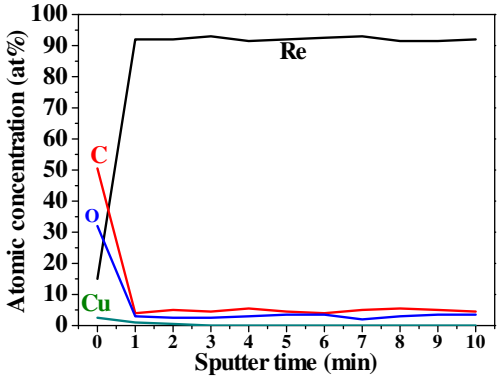

Fig. 8. XPS depth profiles for sample #125.

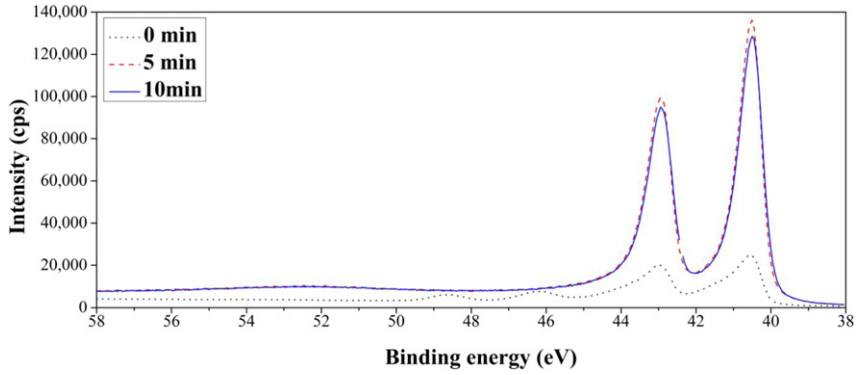

Fig. 9. The Re 4 f XPS spectra from sample #125 before and after sputter cleaning.

oxide was formed at the surface. The concentration of Re was essentially constant during sputtering from 1 to 10 min.

Fig. 9 shows the XPS measurements of sample #125 before and after sputtering. It should be noted that the Re 4 f spectra is composed exclusively of doublet structures due to multiplet splitting ($4f_{5/2}$ and $4\ f_{7/2}$) after sputtering, indicating that the film consisted of the Re state. Curve fitting was conducted to quantify and to deconvolute the contribution of the C and Re elements. Fig. 10 shows high-resolution XPS spectra of sample #125 before sputtering. The C and Re spectra are shown in Fig. 10(a) and (b), respectively. The different states of Re, their quantities, and their peak positions before sputtering are summarized in Table 4. It can be observed from Fig. 10(a) that the states of C includes C-C, C-H, C-O, and NC═O, which originate from the adsorption of organic additives on the surface. These states of organic matter could influence the electrodeposition of the film. The O-C═O and NC═O states result from the gelatin additive (cf. Fig. 10). The peak position of Re oxides is in agreement with those detected in previous works [14,18], with the exception of a new state with chemical bond content of 33.04%. In this study, a doublet with Re 4 $f_{7/2}$ peak at 41.00 eV was detected before sputtering. Its binding energy was higher than that of Re, but lower than that of ReO_2. A new state at ~41.00 eV was also detected by Cohen Sagiv et al. [18] and was related to an oxidized state of Re-alloy + O. In this study, the concentration of Ni in the film was very low, indicating that it may be a new Re-O-C-complex state (cf. Table 4).

The atomic concentrations of the elements after sputtering were somewhat different than those obtained by EDS. This discrepancy may be related to inhomogeneity of the deposit or to non-uniform sputtering [18]. According to the EDS patterns, the coating consists of Re and Cu, the latter indicating a thin film. The elements C, O and N were not detected due to the intrinsic ~1% error limit of the instrument.

3.5. Crystallographic structure

Fig. 11 shows the XRD patterns from Re-rich Re-Ni alloys. When no additive was used (Fig. 11(a)), a broad diffraction peak at ~42.6° indicates that the Re-Ni alloy consists of an amorphous phase. This amorphous

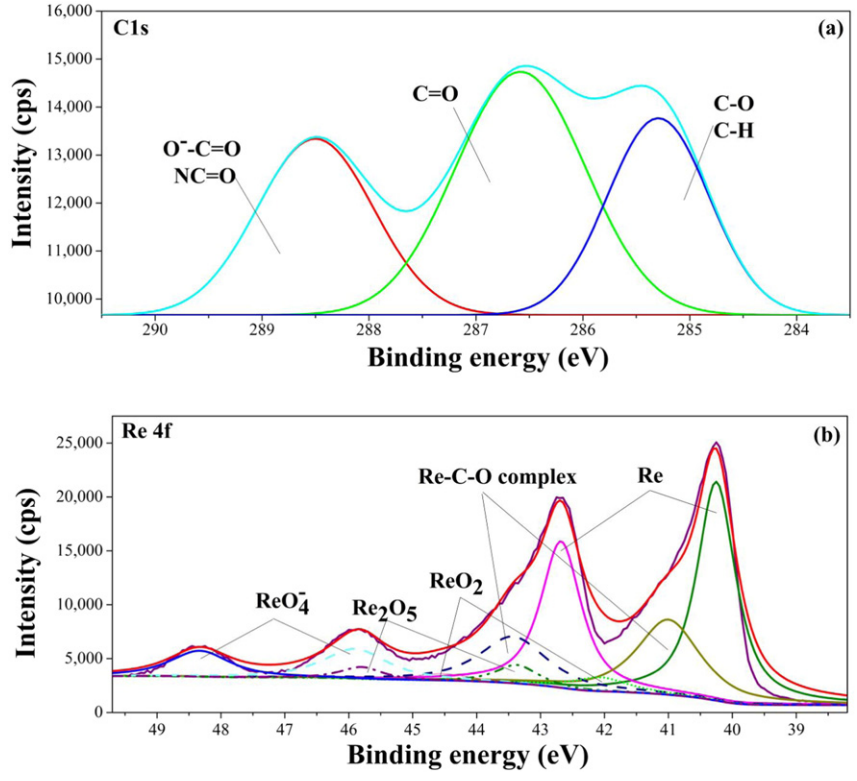

Fig. 10. High-resolution XPS spectra of sample #125 before sputtering. (a) C1s and (b) Re 4 f.

Table 4
Peak positions and relative abundance (% out of at% Re presented in Table 3) of oxidation states of Re at the surface of sample #125 before sputtering.

Component	Peak position	Binding energy (eV)	FWHM (eV)	Chemical bond content (%)	Chemical bond total content (%)
Re	$4f_{7/2}$	40.25	0.72	24.99	43.8
	$4f_{5/2}$	42.68	0.75	18.74	
Re-O-C-complex	$4f_{7/2}$	41.00	1.17	18.88	33.0
	$4f_{5/2}$	43.43	1.25	14.16	
ReO_2	$4f_{7/2}$	42.07	1.05	3.13	5.5
	$4f_{5/2}$	43.43	1.05	2.34	
Re_2O_5	$4f_{7/2}$	43.37	0.78	2.82	4.9
	$4f_{5/2}$	45.80	0.78	2.11	
ReO_4^-	$4f_{7/2}$	45.90	1.22	7.33	12.8
	$4f_{5/2}$	48.33	1.12	5.49	

phase was still evident with the addition of all three additives. Samples #67 and #125 also show the amorphous phase (Fig. 11(b) and (c)). However, the reflections from the copper substrate appear, due to the thin nature of the coating (Fig. 11(c)). For coatings deposited from additives-containing baths, the halo shifts to somewhat lower diffraction angle (~41.6°), indicating an increase in the interatomic spacing. This effect can be attributed to an increase in the Re-content. A similar shift in W-content has been reported by Yamasaki [40] and Hou et al. [41] in the Ni-W system. This was further supported by the XRD results from sample #125 (Re film) deposited with three types of additives (Fig. 11(c)). For the Re film, the halo shifts to somewhat lower diffraction angle (~41°), compared with other halo reflections.

4. Conclusions

We studied the synergistic effect of additives on the properties of Re-Ni electrodeposition, and investigated the effects of bath chemistry and operating conditions on the FE, partial current densities, chemical composition, and surface morphology of Re-rich Re-Ni alloy deposits. The following conclusions were drawn:

Additives were found to have a significant influence on the nature of the deposit. The surface morphology was changed from uniformly smooth without additives to relatively coarse-grained with additives. The deposition rate and crack density decreased when a mixture of additives was present in a bath containing 34 mM ReO_4^-, 124 mM Ni^{2+} and 343 mM Cit^{3-}.

The Re-rich alloys were found to be amorphous. The effect of increased ReO_4^- concentration at varying Ni^{2+} concentrations was explored. At high concentrations (124 and 155 mM) of Ni^{2+}, the Re-content decreased slightly, whereas the FE increased dramatically with increasing concentration of ReO_4^-. In contrast, at low concentrations (34 and 63 mM) of Ni^{2+}, the Re-content was essentially independent of the concentration of ReO_4^-. Likewise, increasing the concentration of ReO_4^- was found to slightly increase the FE, increase the partial current density of Re, and barely affect that of Ni. In the presence of 93 mM of Ni^{2+}, the behavior was intermediate. An increase in the citrate-to-nickel ratio leads to a decrease in the FE and partial current densities of Re and Ni, yet to an increase in the Re-content in the alloy. This is due to the sequestering of Ni^{2+} ions in complexes with $[NiCit_2]^{4-}$. As a result, the rate of Ni deposition is strongly hindered, thus allowing for greater Re-content.

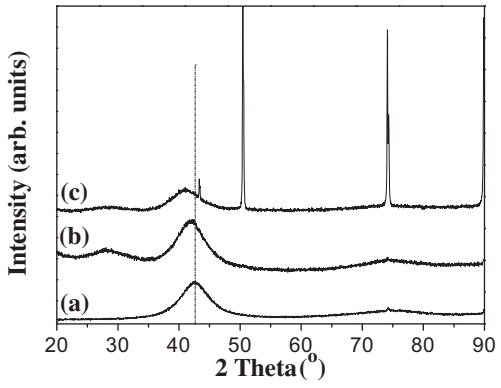

Fig. 11. XRD patterns from Re-Ni coatings deposited without (a) and with additives (b) and (c). The samples are: (a) Ref. [11], (b) #67, (c) #125.

The pH was found to have a significant effect on the properties of the Re-Ni alloys formed. The highest FE and partial current density of Re were obtained at pH = 5, but the Re-content of the alloy was somewhat lower than at pH = 4. An increase in the bath temperature led to an increased FE and Re-content in the deposit, as well as in the partial current density for Re. The partial current density for Ni deposition remained essentially constant regardless of bath temperature. Almost pure Re film was obtained at low concentration of Ni^{2+}, in the presence of additives. A thin layer of Re oxide, a new Re-O-C-complex state and some states of organic matter from the additives were formed at the surface of the Re film, but no cracks were formed. This system may be useful for applications where deposition of very thin films is required.

Acknowledgements

The authors wish to acknowledge partial funding by the U.S. Air Force Office of Scientific Research (AFOSR grant #FA9550-10-1-0520) and the Israel Department of Defense (grant #4440258441). We also thank Dr. Zahava Barkay, Dr. Yuri Rosenberg and Dr. Larisa Burstein from the Wolfson Applied Materials Research Center for their help in ESEM/EDS, XRD and XPS characterization, respectively, and Mr. Mario Levenshtein for his help in the preparation of copper samples and electroplating system apparatus. Dr. Wangping Wu is thankful to the Pikovsky Valazzi fund and to Tel Aviv University for providing him with a postdoctoral scholarship.

References

[1] N. Eliaz, E. Gileadi, Induced codeposition of alloys of tungsten, molybdenum and rhenium with transition metals, in: C.G. Vayenas, R.E. White, M.E. Gamboa-Aldeco (Eds.), Modern Aspects of Electrochemistry, 42, Springer, New York 2008, pp. 191–301.
[2] A. Naor, N. Eliaz, E. Gileadi, S.R. Taylor, Properties and applications of Re and its alloys, The AMMTIAC Quarterly 5 (2010) 11–15.
[3] A.J. Sherman, R.H. Tuffias, R.B. Kaplan, The properties and applications of rhenium produced by CVD, JOM 43 (1991) 20–23.
[4] A. Duhin, A. Inberg, N. Eliaz, E. Gileadi, Electroless plating of rhenium-nickel alloys, Electrochim. Acta 56 (2011) 9637–9643.
[5] A. Duhin, A. Rozenblat-Raz, L. Burstein, A. Inberg, D. Horvitz, Y. Shacham-Diamand, N. Eliaz, E. Gileadi, Growth study of nanoscale Re-Ni coatings on functionalized SiO_2 using electroless plating, Appl. Surf. Sci. 313 (2014) 159–165.
[6] A. Duhin, A. Inberg, N. Eliaz, E. Gileadi, Electroless plating of rhenium-based alloys with nickel, cobalt and iron, Electrochim. Acta 174 (2015) 660–666.
[7] L.E. Netherton, M.L. Holt, Electrodeposition of rhenium-nickel alloys, J. Electrochem. Soc. 98 (1951) 106–109.
[8] V.P. Greco, Rhenium alloys-ion group metals (electrodeposition and properties), Technical Report WVT-7150, Benet R&E Laboratories, Watervliet, NY, 1971.
[9] H. Fukushima, T. Akiyama, M. Shimizu, K. Higashi, Electrodeposition behavior of rhenium-nickel alloys from aqueous solutions, Met. Finish. 35 (1984) 247–251.
[10] H. Fukushima, T. Akiyama, M. Shimizu, K. Higashi, Electrodeposition of Re-Ni alloys from ammoniacal citrate solution, Met. Finish. 36 (1985) 198–203.
[11] A. Naor, N. Eliaz, E. Gileadi, Electrodeposition of rhenium–nickel alloys from aqueous solutions, Electrochim. Acta 54 (2009) 6028–6035.
[12] A. Naor, N. Eliaz, E. Gileadi, Electrodeposition of alloys of rhenium with iron-group metals from aqueous solutions, Electrochem. Soc. Trans. 25 (2010) 137–149.
[13] A. Naor, N. Eliaz, E. Gileadi, Electrodeposition of alloys of rhenium with iron-group metals from aqueous solutions, J. Electrochem. Soc. 157 (2010) D422–D427.
[14] A. Naor-Pomeranz, L. Burstein, N. Eliaz, E. Gileadi, Direct experimental support for the catalytic effect of iron-group metals on electrodeposition of rhenium, Electrochem. Solid-State Lett. 13 (2010) D91–D93.
[15] A. Naor-Pomerantz, N. Eliaz, E. Gileadi, Electrodeposition of rhenium-tin nanowires, Electrochim. Acta 56 (2011) 6361–6370.
[16] P.R. Zabinski, A. Franczak, R. Kowalik, Electrocatalytically active Re-Ni binary alloys electrodeposited with superimposed magnetic field, Arch. Metall. Mater. 57 (2012) 495–501.

[17] F. Contu, S.R. Taylor, Further insight into the mechanism of Re-Ni electrodeposition from concentrated aqueous citrate baths, Electrochim. Acta 70 (2012) 34–41.
[18] M. Cohen-Sagiv, N. Eliaz, E. Gileadi, Incorporation of iridium into electrodeposited rhenium–nickel alloys, Electrochim. Acta 88 (2013) 240–250.
[19] O. Berkh, N. Eliaz, E. Gileadi, The initial stages of electrodeposition of Re-Ni alloys, J. Electrochem. Soc. 161 (2014) D219–D226.
[20] O. Berkh, A. Khatchatouriants, N. Eliaz, E. Gileadi, The influence of weak ionic interactions on electrode reactions during electrodeposition of Re-Ni alloys, J. Electrochem. Soc. 161 (2014) D632–D639.
[21] O. Berkh, L. Burstein, A. Gladkikh, N. Eliaz, E. Gileadi, Characterization of Re-Ni films after the initial stages of electrodeposition, J. Electrochem. Soc. 163 (2016) D295–D299.
[22] B.A. Rosen, E. Gileadi, N. Eliaz, Microstructure and composition of pulse plated Re-Ni alloys on a rotating cylinder electrode, J. Electroanal. Chem. 731 (2014) 93–99.
[23] T. Nusbaum, B.A. Rosen, E. Gileadi, N. Eliaz, Effect of pulse on-time and peak current density on pulse plated Re-Ni alloys, J. Electrochem. Soc. 162 (2015) D250–D255.
[24] B.A. Rosen, E. Gileadi, N. Eliaz, Electrodeposited Re-promoted Ni foams as a catalyst for the dry reforming of methane, Catal. Commun. 76 (2016) 23–28.
[25] W.P. Wu, N. Eliaz, E. Gileadi, The effects of pH and temperature on electrodeposition of Re-Ir-Ni coatings from aqueous solutions, J. Electrochem. Soc. 162 (2015) D20–D26.
[26] S.I. Baik, A. Duhin, P.J. Phillips, R.F. Klie, E. Gileadi, D.N. Seidman, N. Eliaz, Atomic-scale structural and chemical study of columnar and multilayer Re-Ni electrodeposited thermal barrier coating, Adv. Eng. Mater. 18 (2016) 1133–1144.
[27] S.R. Wen, The Electrodeposition and Property Study of Nickel-Rhenium Alloys, Louisiana State University, M.Sc. thesis, 2005.
[28] C.H. Huang, J.R. Jan, W.Y. Shu, H.M. Wu, The sulfur-enhanced effect of absorbing hydrogen in electroformed nickel–rhenium alloy, Mater. Chem. Phys. 70 (2001) 168–174.
[29] D.R. Gabe, The role of hydrogen in metal electrodeposition processes, J. Appl. Electrochem. 27 (1997) 908–915.
[30] N. Eliaz, T.M. Sridhar, E. Gileadi, Synthesis and characterization of nickel tungsten alloys by electrodeposition, Electrochim. Acta 50 (2005) 2893–2904.
[31] M.E. Soares, C.A.C. Souza, S.E. Kuri, Characteristics of a Zn-Ni electrodeposited alloy obtained from controlled electrolyte flux with gelatin, Mater. Sci. Eng. A 402 (2005) 16–21.
[32] O.Y. Zelenin, Interaction of the Ni^{2+} ion with citric acid in an aqueous solution, Russ. J. Coord. Chem. 33 (2007) 346–350.
[33] P.R. Zabinski, A. Franczak, R. Kowalik, Electrodeposition of functional Ni-Re alloys for hydrogen evolution, Electrochem. Soc. Trans. 41 (2012) 39–48.
[34] N. Eliaz, K. Venkatakrishna, A.C. Hegde, Electroplating and characterization of Zn–Ni, Zn–Co and Zn–Ni–Co alloys, Surf. Coat. Technol. 205 (2010) 1969–1978.
[35] M. Paunovic, M. Schlesinger, Fundamentals of Electrochemical Deposition, second ed. John Wiley & Sons, 2005 177–198.
[36] İ.H. Karahan, Effects of pH value of the electrolyte and glycine additive on formation and properties of electrodeposited Zn-Fe coatings, The Scientific World J. (2013), 273953.
[37] T.C. Franklin, Some mechanisms of action of additives in electrodeposition processes, Surf. Coat. Technol. 30 (1987) 415–428.
[38] G.M. Brown, G.A. Hope, SERS study of the adsorption of gelatin at a copper electrode in sulfuric acid solution, J. Electroanal. Chem. 397 (1995) 293–300.
[39] N.A. Kostromina, S.L. Davydova, A.D. Shaposhnikova, V.P. Tikhonov, PMR investigation of gelatin and its complex formation with nickel and cobalt, Theor. Exper. Chem. 15 (1979) 228–233.
[40] T. Yamasaki, High-strength nanocrystalline Ni-W alloys produced by electrodeposition and their embrittlement behaviors during grain growth, Scr. Mater. 44 (2001) 1497–1502.
[41] K.H. Hou, Y.F. Chang, S.M. Chang, C.H. Chang, The heat treatment effect on the structure and mechanical properties of electrodeposited nano grain size Ni–W alloy coatings, Thin Solid Films 518 (2010) 7535–7540.